Supplement of Atmos. Chem. Phys., 21, 16277–16291, 2021
https://doi.org/10.5194/acp-21-16277-2021-supplement

Atmospheric Chemistry and Physics
Open Access
EGU

Supplement of

Changes in biomass burning, wetland extent, or agriculture drive atmospheric NH_3 trends in select African regions

Jonathan E. Hickman et al.

Correspondence to: Jonathan E. Hickman (jonathan.e.hickman@nasa.gov)

Contents of this file

Text S1 to S2
Figures S1 to S20
Table S1

Introduction

The supporting information contains four main categories of supporting information. First, Figures S1-S5, S7, S11, and S20 represent additional continental-scale figures supporting analysis in the main text of the document. Figure S6 provides supporting analysis of trends in West Africa. Text S1 and Figures S8-S10 and S12 provides supporting analysis of trends in South Sudan, including the potential effects of conflict in South Sudan. Figures S13-S18 provide supporting analysis of trends in the Lake Victoria region. Figure S19, Table S1, and Text S2 provide supporting analysis of national-scale relationships. Collection, generation, processing, and analysis of data are described either in the main document or in the relevant supplementary text section.

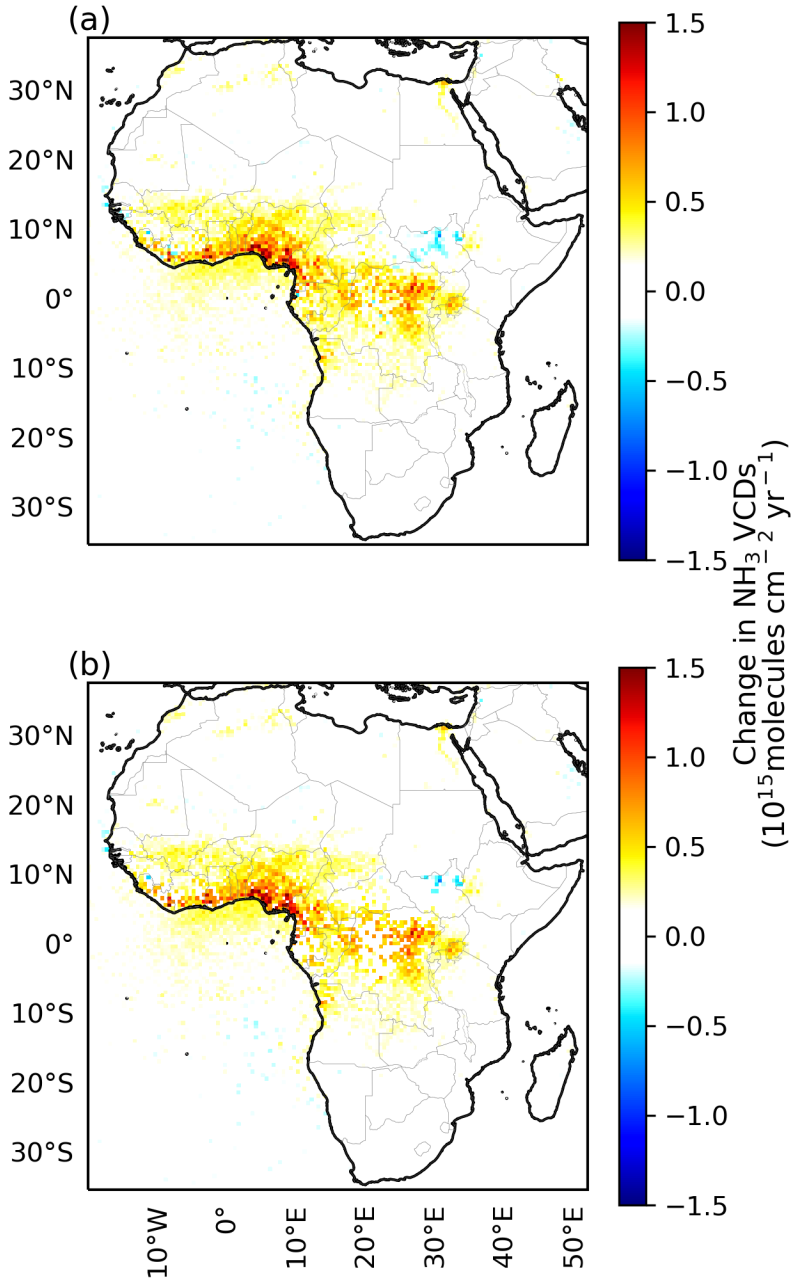

Figure S1. Trend in atmospheric NH_3 VCDs from IASI for the period 2008 through 2018 where trends meet the significance threshold of (a) p=0.05 or (b) p=0.20.

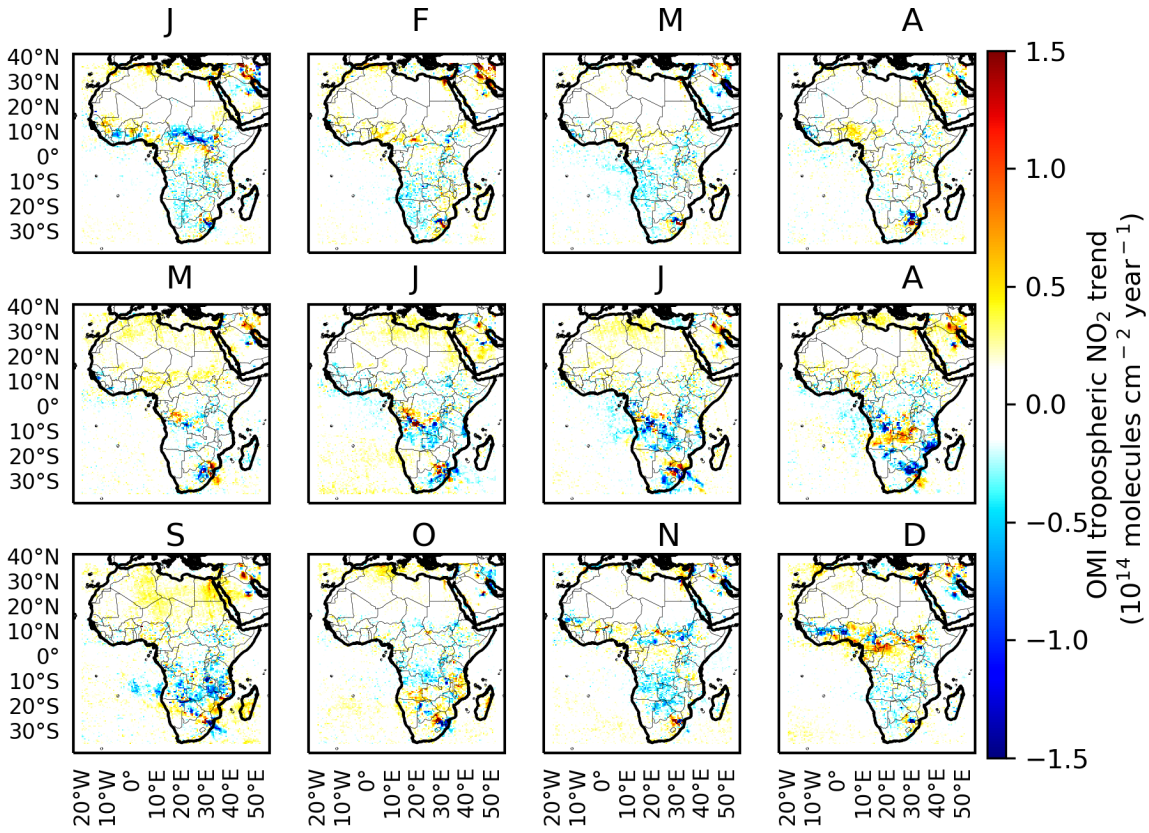

Figure S2. Change in mean monthly atmospheric OMI NO_2 VCDs for the period 2008 through 2018.

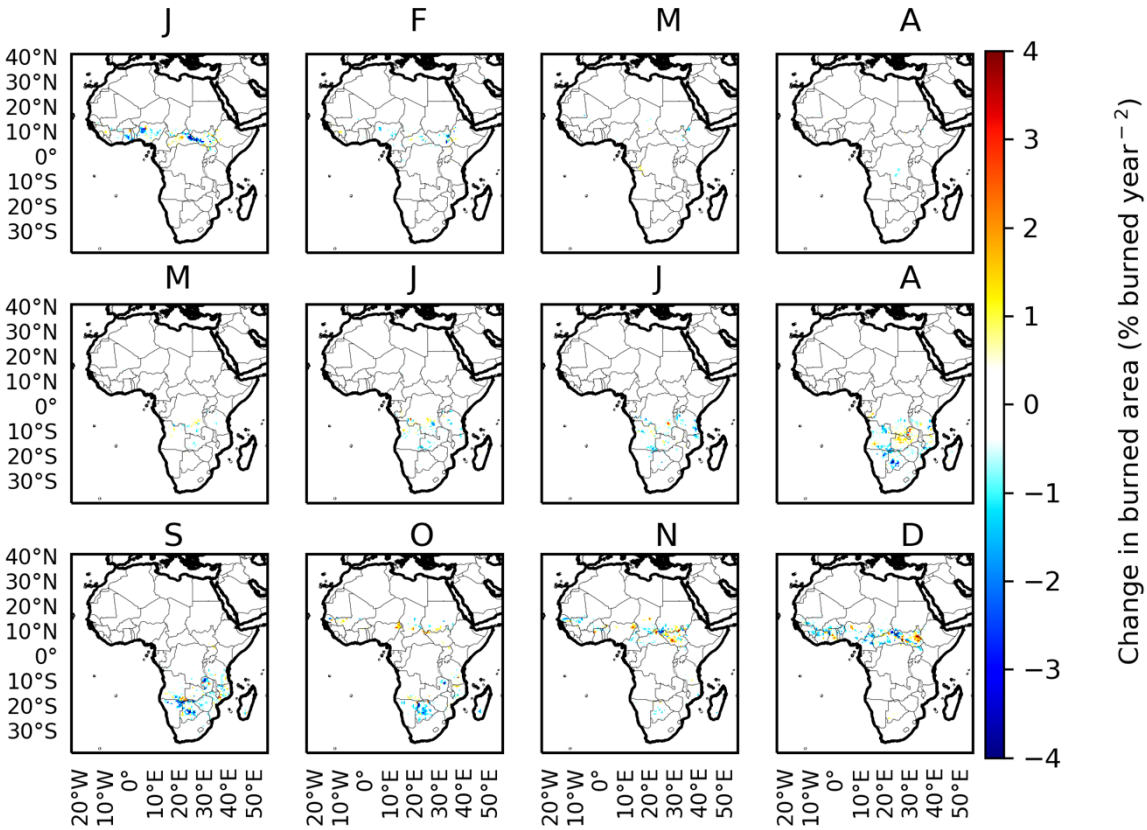

Figure S3. Change in mean monthly atmospheric MODIS burned area for the period 2008 through 2018.

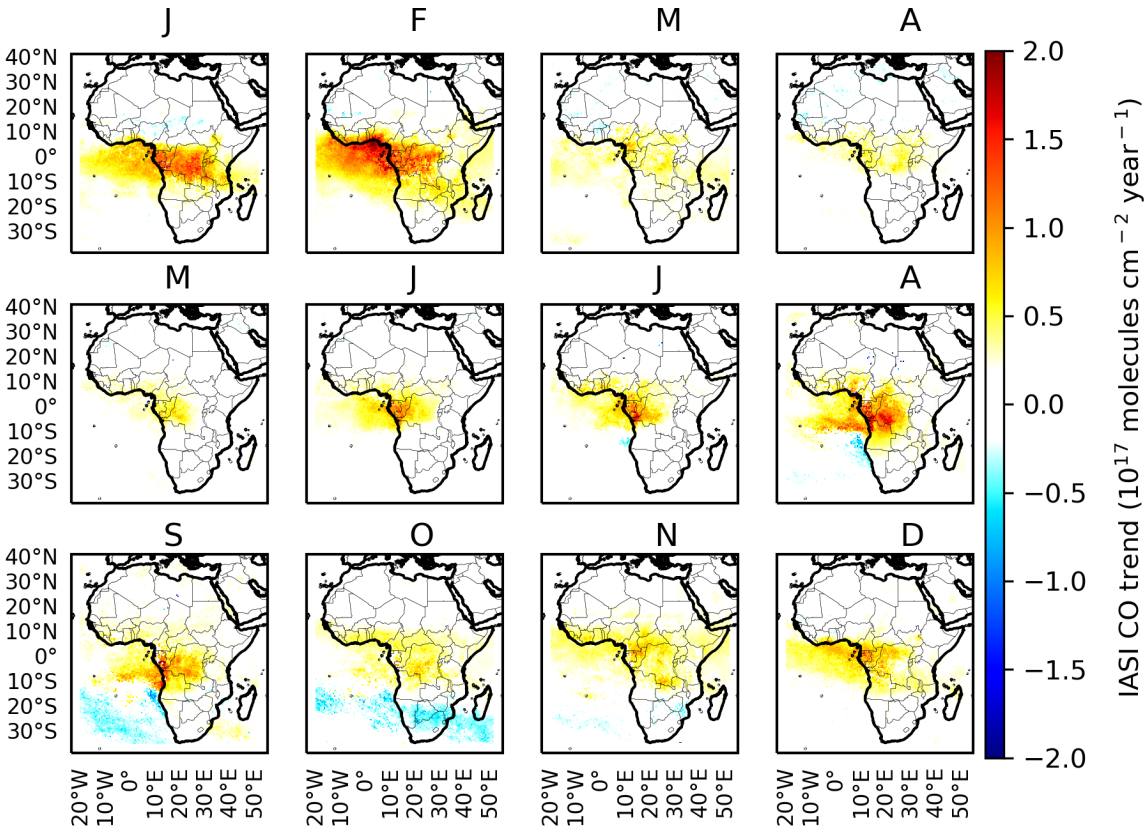

Figure S4. Change in mean monthly atmospheric CO VCDs for the period 2008 through 2018.

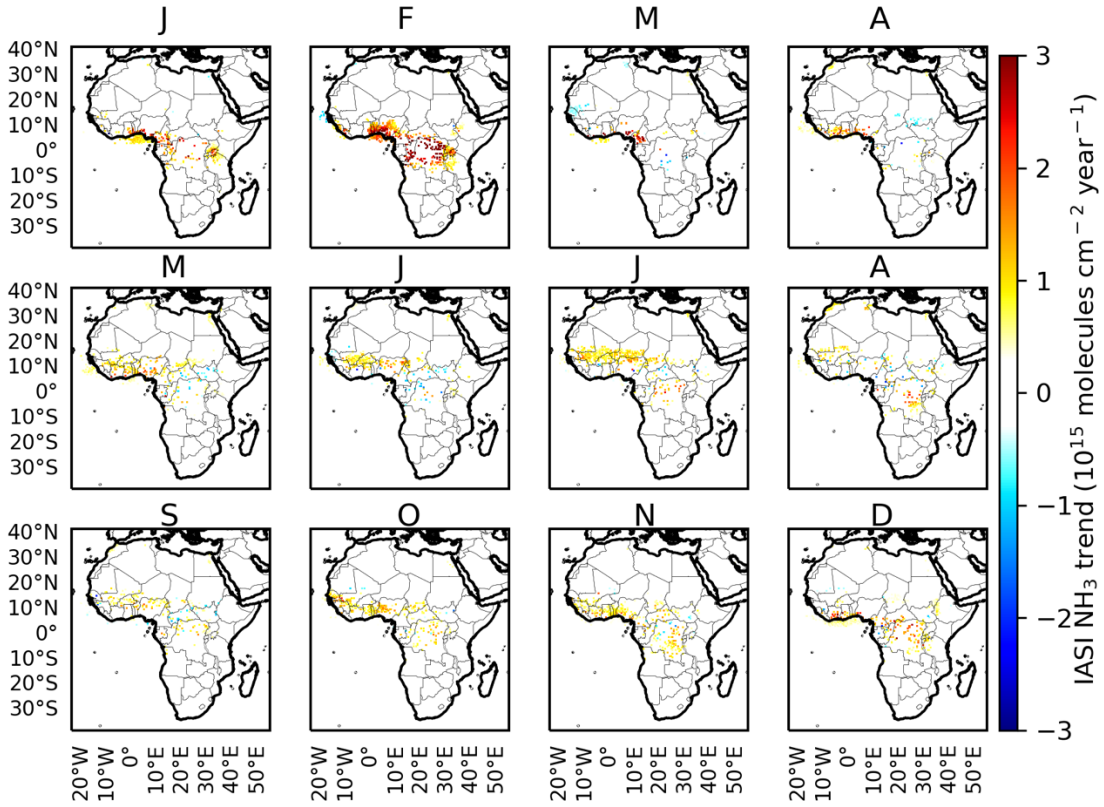

Figure S5. Change in mean monthly atmospheric NH_3 VCDs for the period 2008 through 2018 where the relationship is significant at p=0.05. Grid cells where mean annual NH_3 VCDs for the entire period are under $5x10^{15}$ molecules cm^{-2} are not displayed.

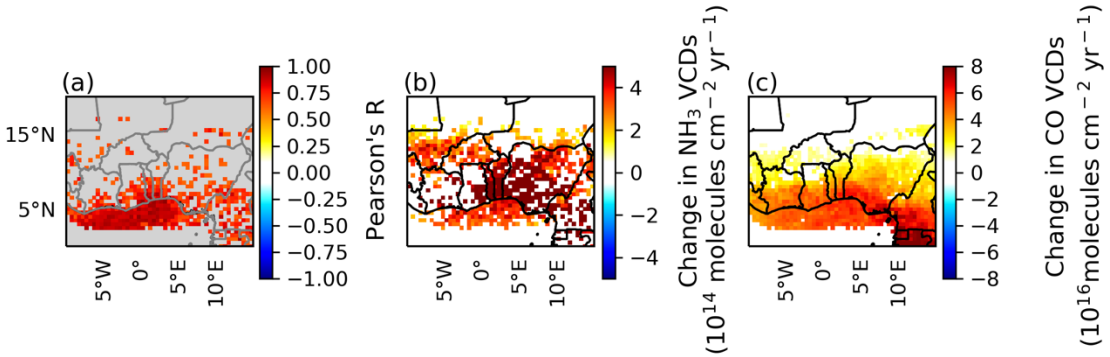

Figure S6. Correlation coefficient for the relationship between mean annual CO and NH_3 VCDs (a), changes in NH_3 VCDs (b) and changes in CO VCDs (c) over 2008 through 2018 in West Africa where the relationship is significant at p=0.05. Grid cells where mean annual NH_3 VCDs for the entire period are under $5x10^{15}$ molecules cm^{-2} are not displayed.

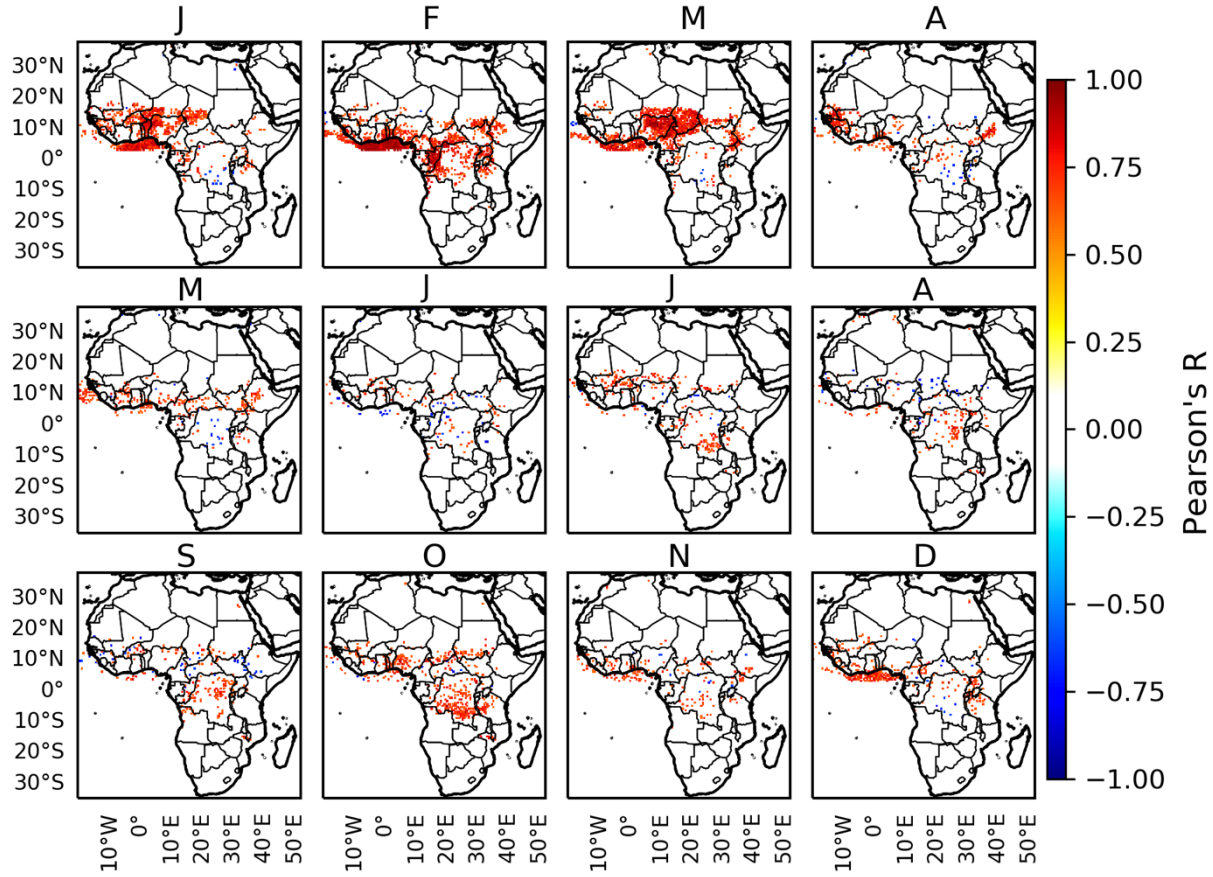

Figure S7. Correlation coefficient for the relationship between mean annual CO and NH_3 VCDs over 2008 through 2018 where the relationship is significant at P=0.05. Regions where mean annual NH_3 VCDs for the entire period are under $5x10^{15}$ molecules cm^{-2} are screened out.

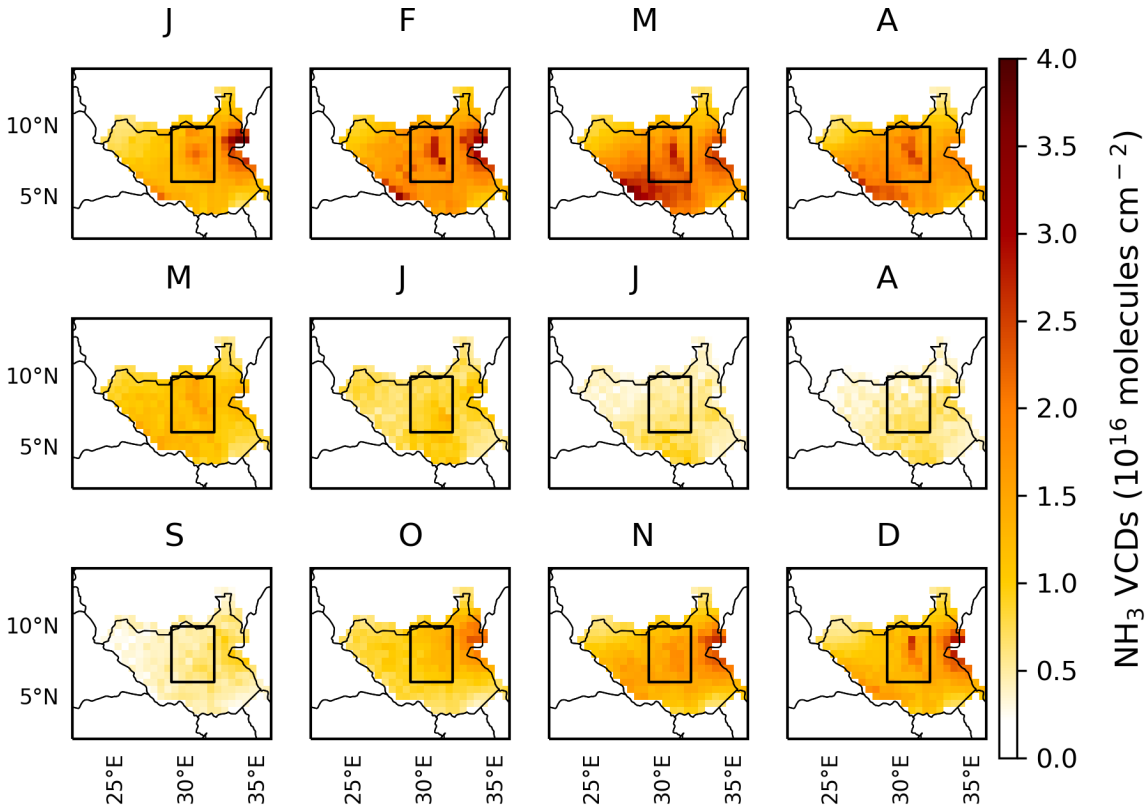

Figure S8. Mean monthly atmospheric NH_3 VCDs over South Sudan; mean is for the period 2008 through 2018.

Text S1. South Sudan conflict

In 2013, a civil conflict emerged in South Sudan that was ultimately responsible for the displacement of millions of people (Global Internal Displacement Monitoring Centre, 2020; World Bank, 2019) and the disruption of livestock migration patterns (Idris, 2018). These disruptions could be expected to lead to a decrease in NH_3 VCDs if they result in lower rates of fertilizer use and a decrease in livestock and livestock-related emissions. Although there are some spatial correspondences between the location of conflict events and changes in NH_3 VCDs (Fig. S7), the change in NH_3 VCDs appears already to have been underway years in advance of the onset of conflict (Fig. S6, Fig. S8), suggesting that other factors are responsible for the interannual variation. Displacement spiked in 2014, the year that NH_3 VCDs were at their lowest values. It is possible that this displacement and the associated conflict contributed to the low NH_3 values, but 2014 was the year of the largest Sudd extent during February through May, which would also be expected to reduce NH_3 emissions. The number of refugees and internally displaced people increased substantially from 2013 through 2017, a period during which the dry season flooded extent of the Sudd decreased, and NH_3 VCDs increased (Fig. S8). Maps of trends and annual mean NH_3 VCDs over the IASI lifetime reveal that most interannual variability occurs over the Sudd (Fig. S7, S10). The strong spatial relationship between the Sudd and interannual NH_3 variability suggests that Sudd flooded extent is likely the main factor responsible for the interannual variation in NH_3 VCDs during this period, and the overall trend we observe for 2008 through 2017.

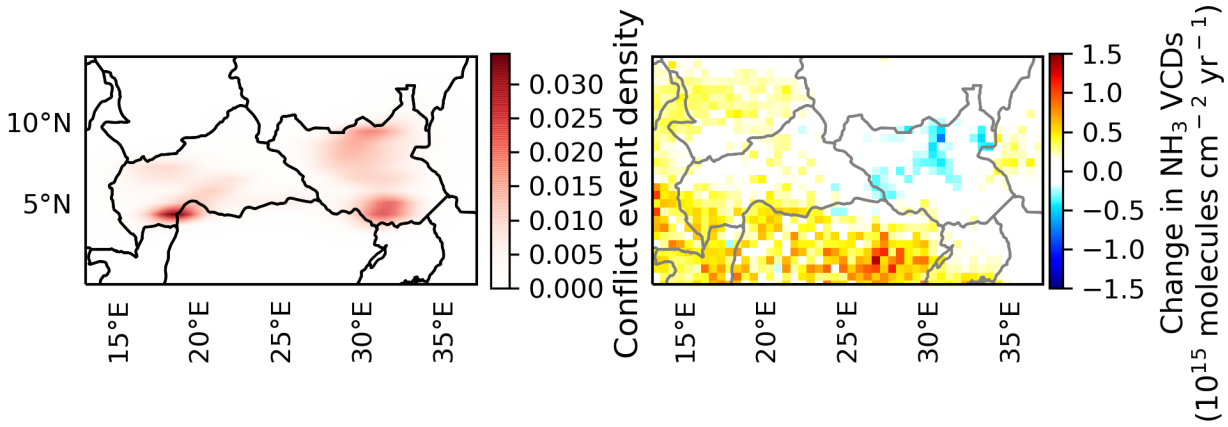

Figure S9. Kernel density estimate of conflict events (left) and change in NH_3 concentrations (right) between 2008 and 2018. Conflict data are from the Armed Conflict Location and Event Project (Raleigh et al., 2010; acleddata.com), and includes both violent and non-violent events.

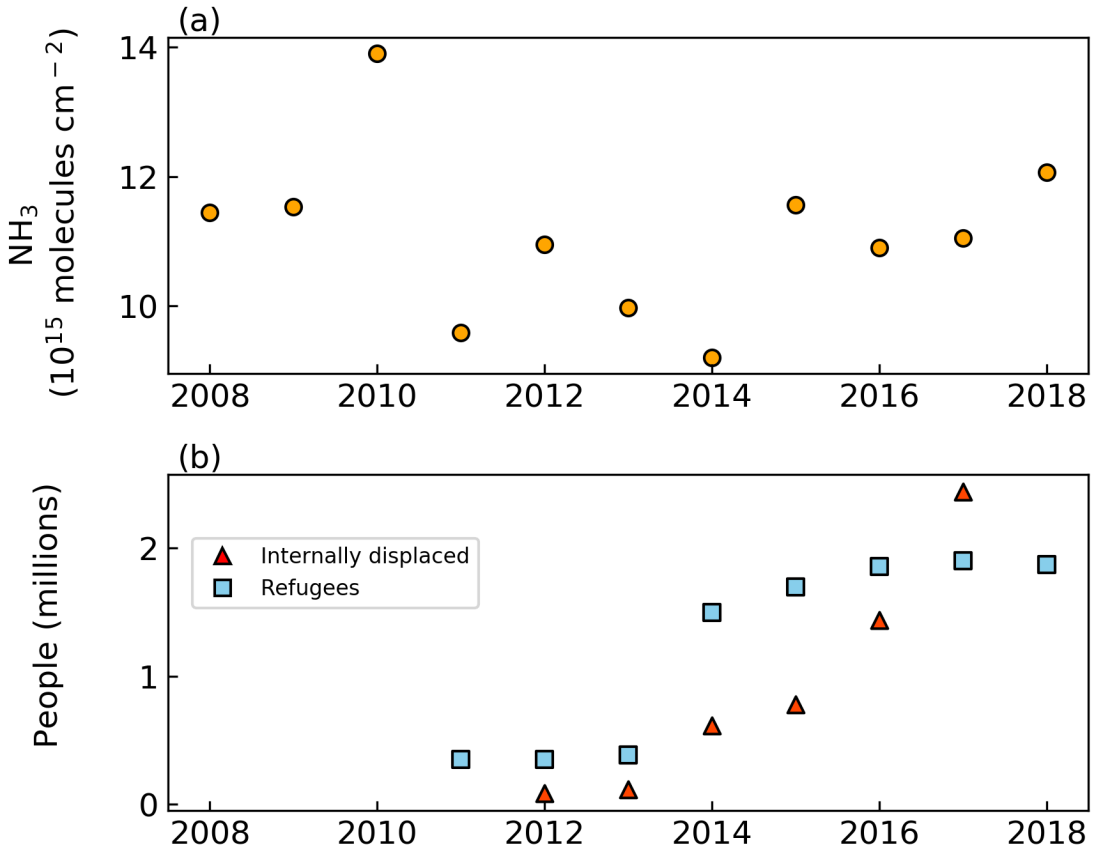

Figure S10. Mean annual NH3 VCDs (a) and mean annual refugees and internally displaced people (b) in South Sudan over the 2008-2018 period for years where data are available.

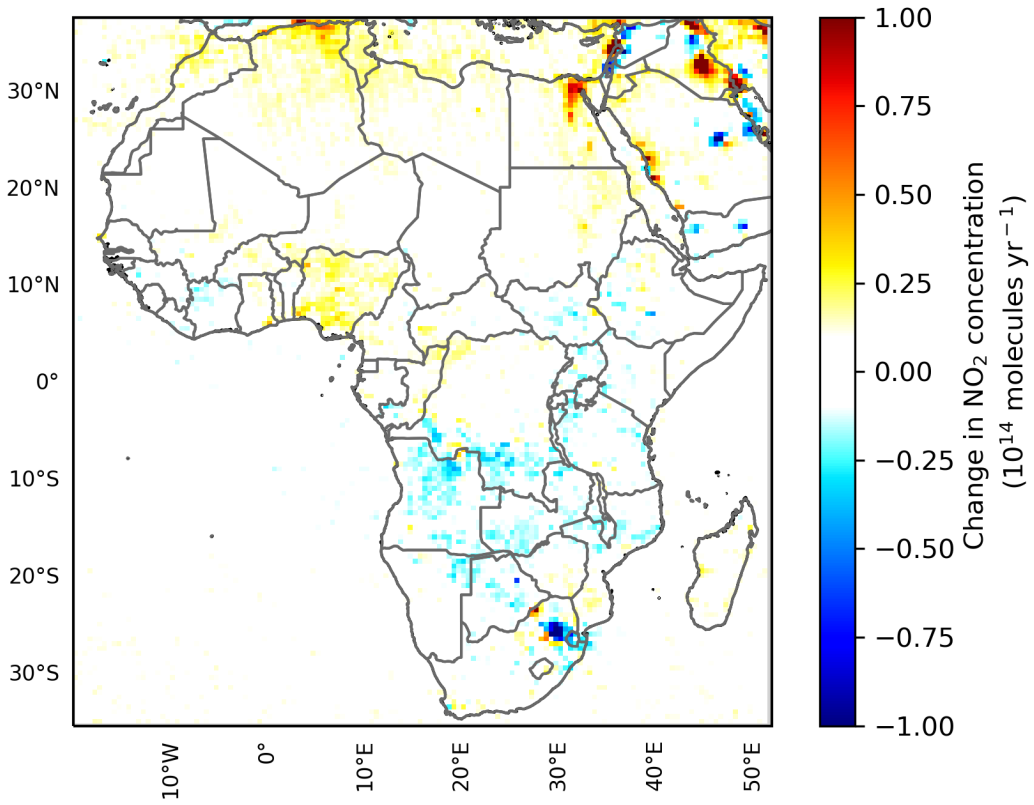

Figure S11. Change in mean annual tropospheric NO_2 VCDs over Africa, 2008 through 2018.

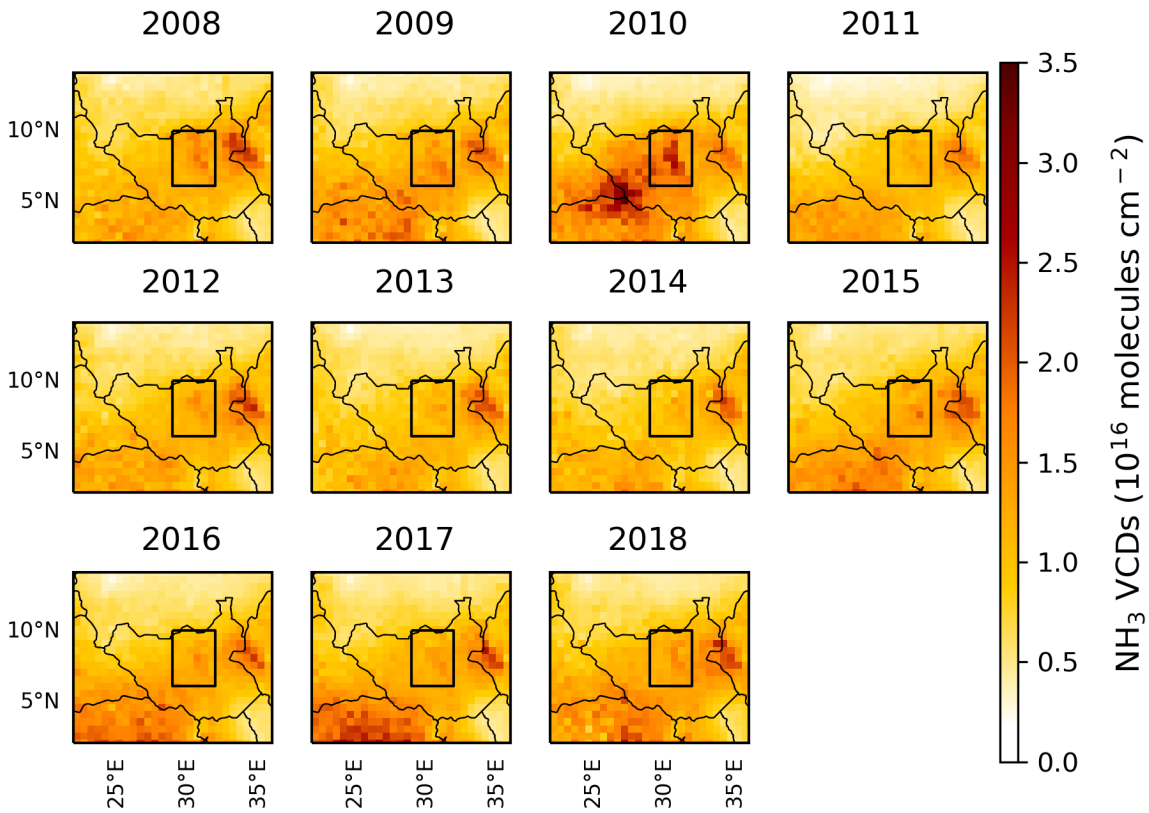

Figure S12. Mean annual atmospheric NH_3 VCDs over South Sudan for 2008 through 2018. The Sudd is highlighted in the black box.

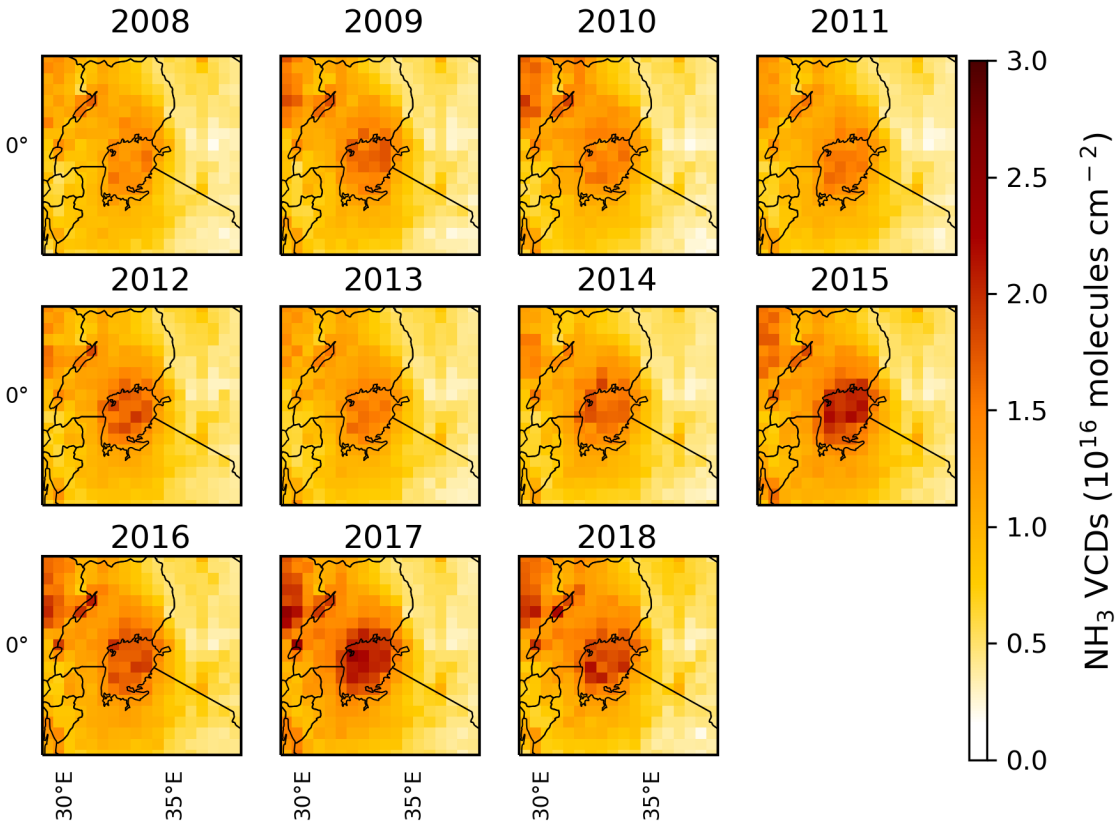

Figure S13. Mean annual atmospheric NH_3 VCDs over the Lake Victoria region for 2008 through 2018.

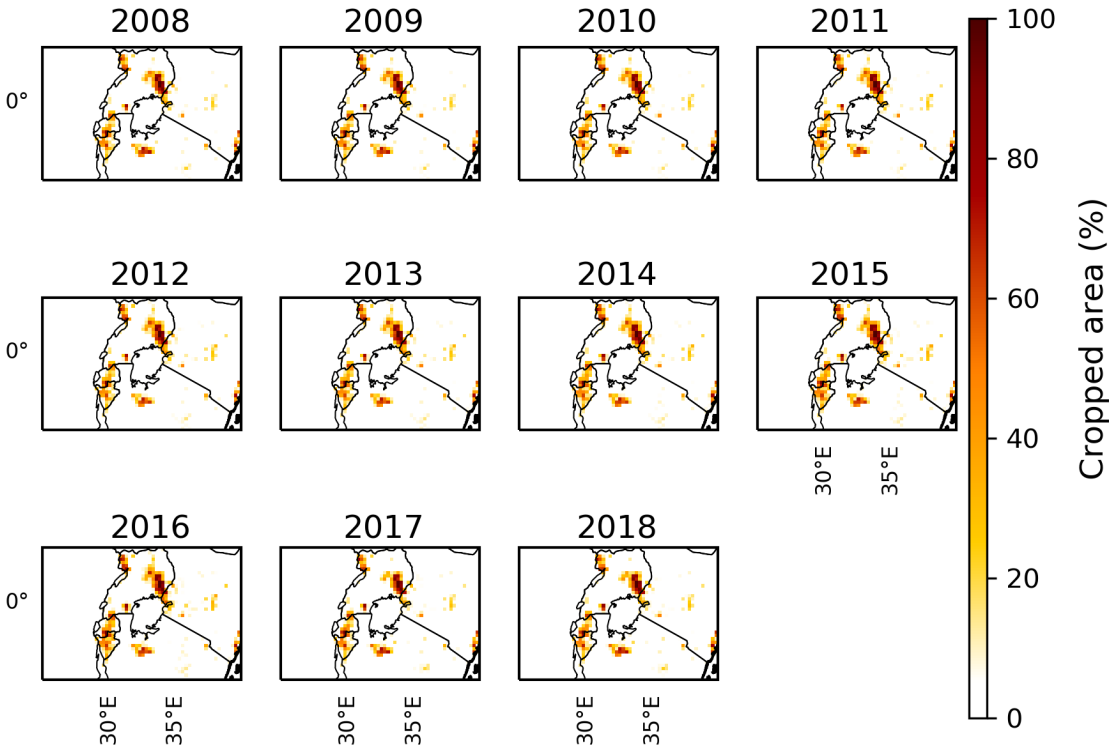

Figure S14. Cropped area in the Lake Victoria region for 2008 through 2018.

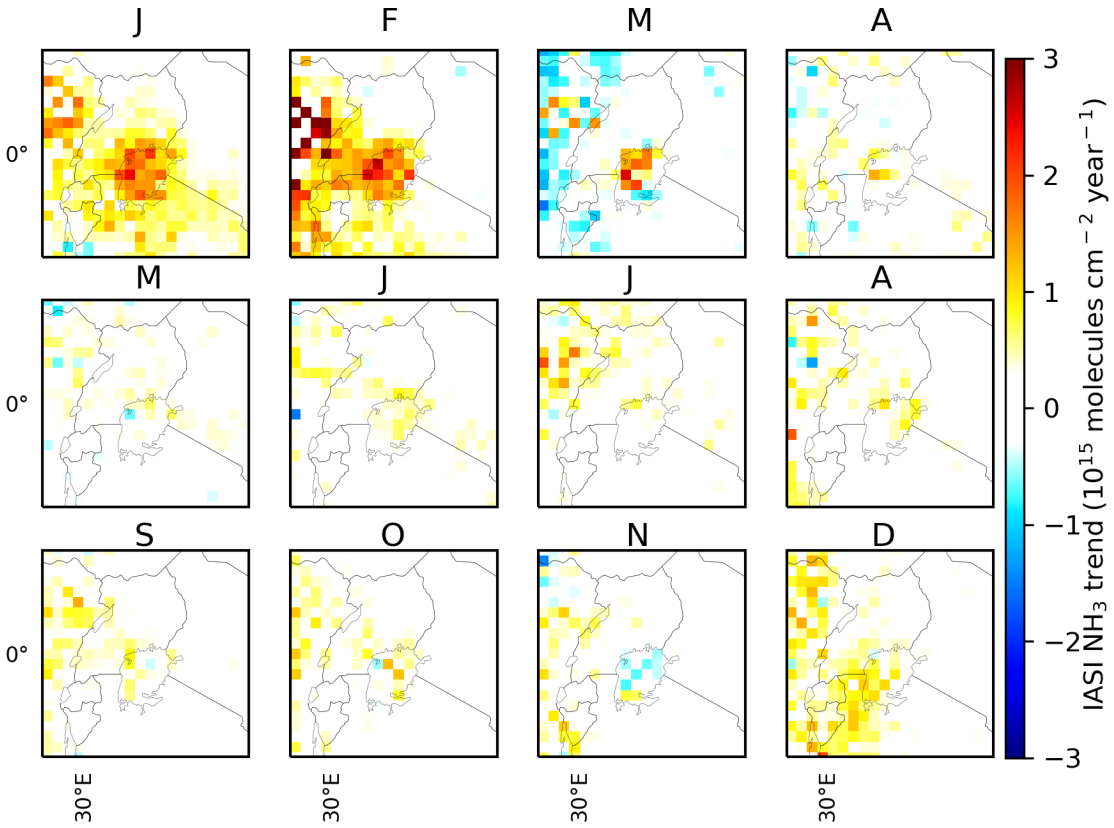

Figure S15. Change in mean monthly atmospheric NH_3 VCDs for the period 2008 through 2018.

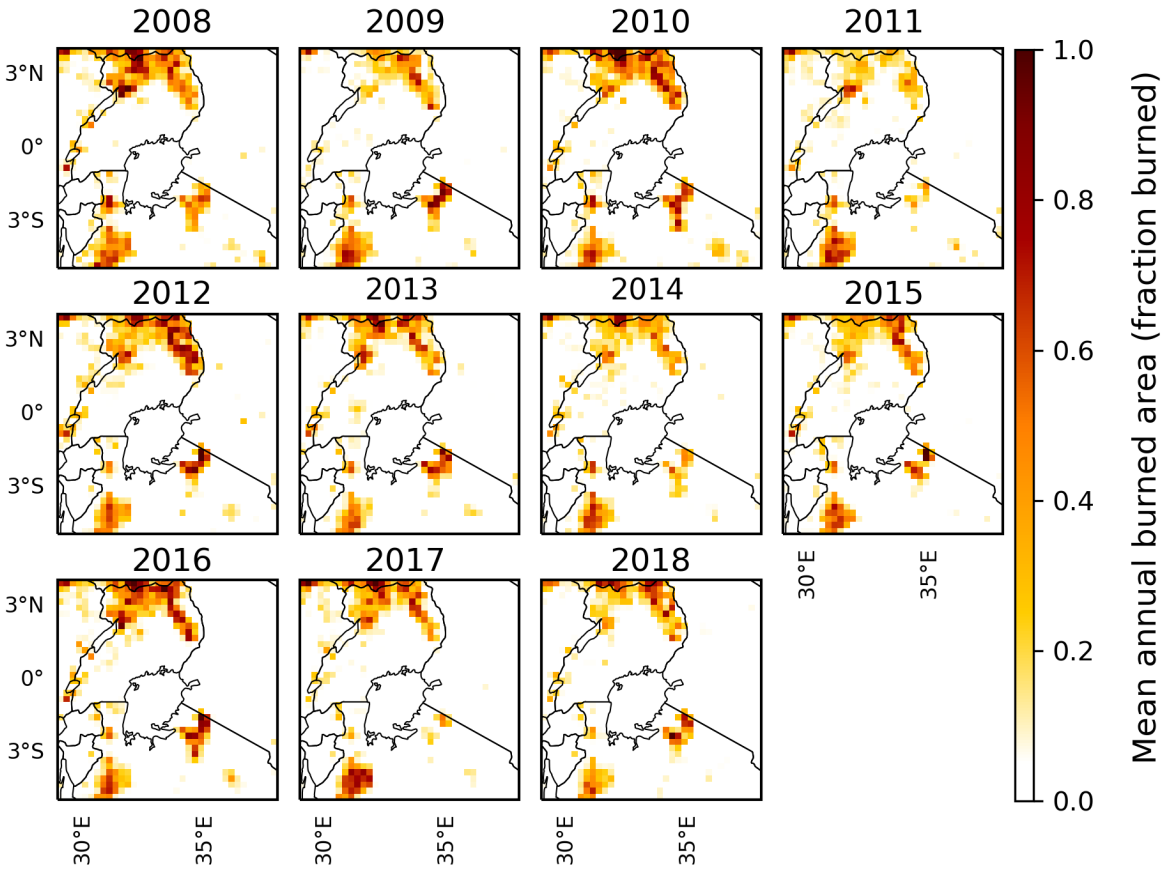

Figure S16. Total annual burned area in the Lake Victoria region for 2008 through 2018.

Figure S17. Mean annual (a) and mean monthly (b) NH_3 VCDs over Lake Victoria and the surrounding land area, 2008-2018.

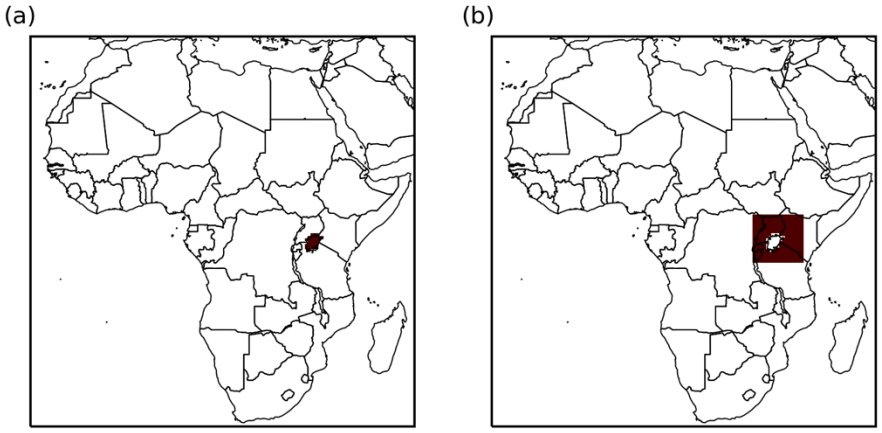

Figure S18. Masks used in time series analysis of NH3 over Lake Victoria (a) and over the surrounding land surface (b).

Text S2. Additional national-scale relationships

Temperature: Mean temperature changes are small—less than 0.015% yr-1 with standard errors that bracket zero; the values are too small to appear on Figure S19. Although they are nearly significantly different among bins at p=0.11 , they do not exhibit a relationship with NH_3 at the country scale in our binned analysis: the annual rate of warming is lowest in the middle bin (0.006 C yr^{-1}) and roughly equal in the bottom and top bins (0.013 C yr^{-1} and 0.017 C yr^{-1}, respectively).

NO_2: NO_2 exhibits marginal increases in each bin, which appear to decrease across bins, but these differences are not significant (Fig. S19; p=0.55). It remains possible that changes in NO_2 emissions may influence NH_3 trends by decreasing the lifetime of NH_3 in the atmosphere, which would be evident as a negative correlation between the two species. In examining spatial relationships between the two gases there is a lot of noise (Fig. S20), but in Nigeria, South Sudan, the Nile Region, and the North African coast, we observe positive correlations, suggestive that changes in NH_3 VCDs in those regions are not the result of reactions with NO_2. Instead, the fact that trends of both gases have the same sign is consistent with changes in emissions being responsible for the trends.

SO_2: As with NO_2, SO_2 may be expected to decrease the lifetime of NH_3. However, in our binned analysis, SO2 did not vary among bins (Fig. S19; p=0.98). In addition, NH_3 and SO_2 may vary increase in parallel, suggesting that chemistry involving SO_2 does not make an important contribution to the observed NH_3 trends. Outside of South Africa, variation in SO_2 emissions in sub-Saharan Africa are largely related to volcanic emissions. During the period of our analyses, emissions from volcanoes in eastern Democratic Republic of Congo and Eritrea play particularly important roles in interannual SO_2 variability. A 2011 eruption in Eritrea results in an overall decline in SO_2 concentrations in the region in our analysis. In South Africa, SO_2 emissions from an array of coal fired power plants in the highveld have declined over the period of our analyses. However, the variation in SO_2 VCDs is not spatially related to variation in NH_3 VCDs, which are also small in the continental context. Note that we exclude Lesotho from these analyses, which experienced a 1000% rate of increase in SO_2 VCDs from 2005 to 2018; including Lesotho results in a very high mean rate of SO_2 increase in the middle bin.

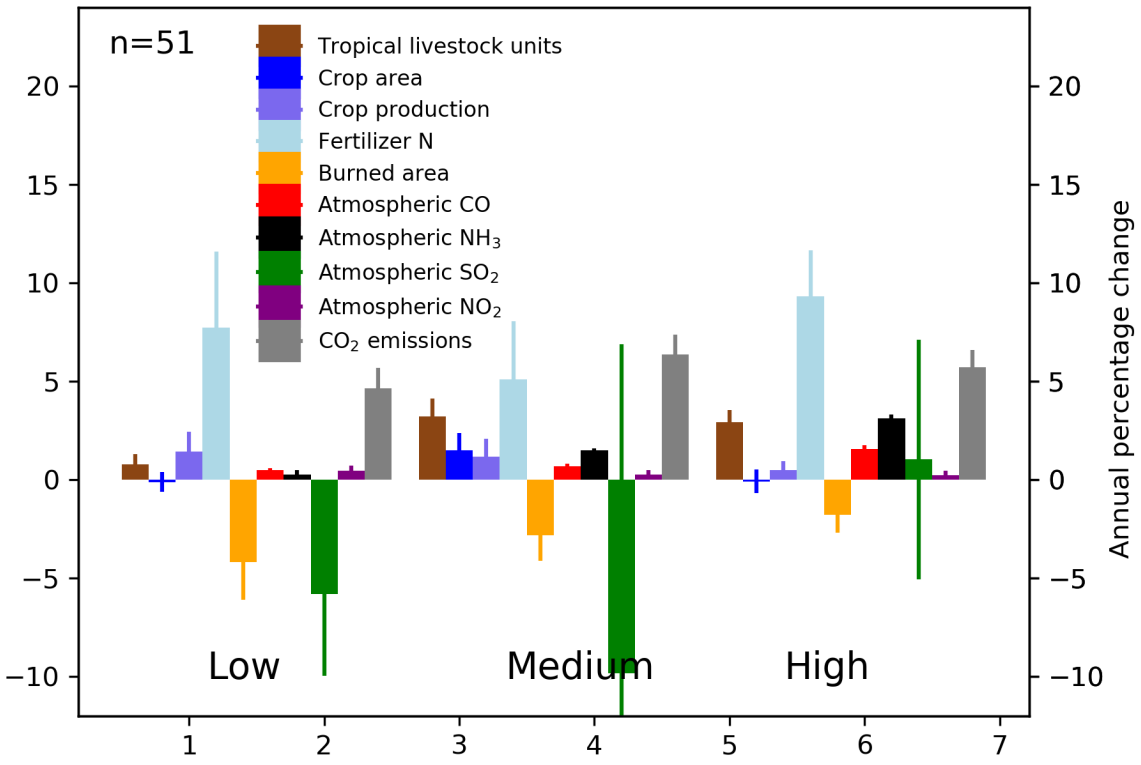

Figure S19. Annual percentage changes in national mean annual Tropical Livestock Units, crop area, crop yield, fertilizer N use, burned area, CO VCDs, NH_3 VCDs, SO_2 VCDs, NO_2 VCDs, and CO_2 emissions for African countries with low, medium, or high rates of NH_3 VCD change for the period 2008-2018. Error bars represent the standard error of the mean. See Table S1 for the list of countries in each bin.

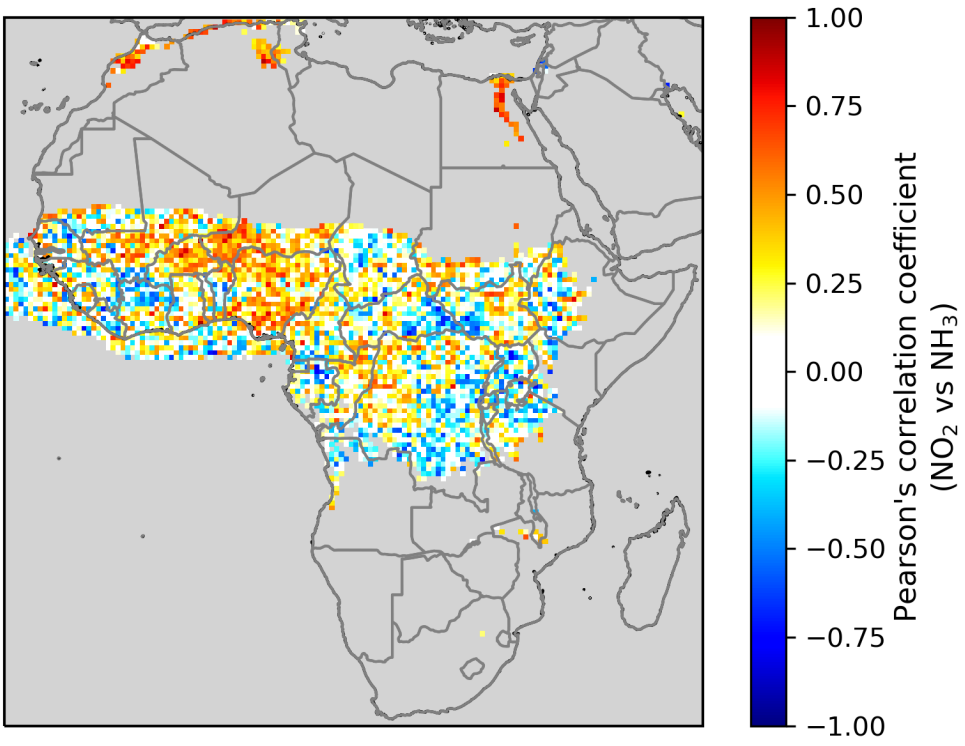

Figure S20. Correlation between mean annual NH_3 and NO_2 VCDs over Africa for the period 2008 through 2018. Pixels where mean annual NH_3 VCDs are below 5 x 10^{15} molecules cm^{-2} for all years are masked.

Table S1. List of countries in Low, Medium, and High bins in Figure 8.

Low bin	Medium Bin	High Bin
Algeria	Central African Republic	Angola
Botswana	Chad	Benin
Djibouti	Cote d'Ivoire	Burkina Faso
Eritrea	Guinea	Burundi
Ethiopia	Kenya	Cameroon
Gambia	Lesotho	Congo
Guinea-Bissau	Liberia	DRC
Libya	Mali	Egypt
Madagascar	Mauritania	Equatorial Guinea
Namibia	Morocco	Gabon
Niger	Mozambique	Ghana
Somalia	Senegal	Malawi
South Africa	Sierra Leone	Nigeria
South Sudan	Sudan	Rwanda
Former Sudan	Tunisia	Tanzania
Eswatini	Uganda	Togo
Western Sahara	Zimbabwe	Zambia

References

Global Internal Displacement Monitoring Centre: Global Internal Displacement Database, [online] Available from: https://www.internal-displacement.org/database/displacement-data, 2020.

Idris, I.: Livestock and conflict in South Sudan - K4D Helpdesk Report 484, Brighton. [online] Available from: https://assets.publishing.service.gov.uk/media/5c6abdec40f0b61a22792fd5/484__Livestock_and_Conflict_in_South_Sudan.pdf, 2018.

Raleigh, C., Linke, A., Hegre, H. and Karlsen, J.: Introducing ACLED: An Armed Conflict Location

and Event Dataset: Special Data Feature, J. Peace Res., 47(5), 651–660, doi:https://doi.org/10.1177/0022343310378914, 2010.

World Bank: World Bank Open Data, World Bank Open Data [online] Available from: https://www.data.worldbank.org (Accessed 2 February 2019), 2019